



# Deformation behavior of bulk nanocrystalline Fe<sub>88</sub>Si<sub>12</sub> alloy

Licai Fu\*, Jun Yang, Qinling Bi, Weimin Liu

State Key Laboratory of Solid Lubrication, Lanzhou Institute of Chemical Physics, Chinese Academy of Sciences, Lanzhou 730000, PR China

## ARTICLE INFO

### Article history:

Received 29 July 2009

Received in revised form 16 October 2009

Accepted 19 October 2009

Available online 27 October 2009

### Keywords:

Nanocrystalline

Mechanical behavior

Deformation mechanism

## ABSTRACT

The deformation behavior of bulk nanocrystalline Fe<sub>88</sub>Si<sub>12</sub> alloy has been investigated with compression tests at different strain rates. The activity volume  $v^*$  is  $6b^3$  which indicates that the deformation mechanism is controlled by the dislocation slip. On the other hand, the critical size of the nanocrystalline Fe<sub>88</sub>Si<sub>12</sub> alloy for deformation mechanism is calculated to be about 5.3 nm. It is smaller than the grain size of the nanocrystalline Fe<sub>88</sub>Si<sub>12</sub> alloy (10 nm), which also indicates that deformation mechanism of the nanocrystalline Fe<sub>88</sub>Si<sub>12</sub> alloy is controlled by the dislocation pile-up.

© 2009 Elsevier B.V. All rights reserved.

## 1. Introduction

Mechanical behavior of nanocrystalline metals and alloys has attracted considerable attention in recent years, due to their high yield and fracture strength, which exhibits large potential for structural applications. But the lower room temperature ductility than their coarse grained counterparts seriously hinders their full potential applications. In order to improve the room temperature ductility, a number of methods have been investigated in the recent decades [1–3], such as bimodal grain size distribution, second phase composite, nano-twin strengthen, strain rate change. For conventional metals and alloys, plastic deformation occurs by dislocation activities. However, dislocation nucleation from the Frank–Read source becomes difficult when the grain size reduces to the nanometer magnitude. Therefore, lots of investigations suggest that the deformation mechanism changes from slip involving perfect dislocations to slip involving shockley partial dislocations, to grain boundary slip deformation at the very small grain size [4–8].

Large numbers of experimental evidences point to the critical size and the critical shear stress additional mechanical characteristic of nanocrystalline metal and alloy [5,9,10]. A transition from deformation mechanisms controlled by dislocation slip to partial dislocation activity carries out when the grain size decreases to the critical grain size. According to the classical dislocation theory, Cheng et al. [11] used a simple model to estimate the critical grain size  $d_c$  and the critical shear stress  $\tau_c$  and predicted the strength of 3 GPa for iron, which was almost exactly what has been measured by Malow and Koch [12]. The transition also has been approved by many molecular–dynamics simulations [9,13]. For explaining how

the grain boundary slip mechanism has been actualized, the strain rate sensitivity (SRS) and the activation volume were related. The SRS is an order of magnitude higher for nanocrystalline metals than for coarse counterpart [14,15]. Moreover, the activation volume is two orders of magnitude smaller for nanocrystalline metals than for coarse counterpart [16].

Fe<sub>88</sub>Si<sub>12</sub> (ratio of atom) alloy is a very suitable material for electrical devices due to its enhanced magnetic properties. Nevertheless, the well-known poor ductility of Fe–Si alloy above 3 wt% Si has blocked mass production by conventional rolling schedules. It is necessary to research the deformation behavior of the nanocrystalline Fe<sub>88</sub>Si<sub>12</sub> alloy, and to expose the deformation mechanism of the nanocrystalline Fe<sub>88</sub>Si<sub>12</sub> alloy, which obtains the methods to improve the ductility of the high Si content Fe–Si alloy.

## 2. Experimental

The bulk nanocrystalline Fe<sub>88</sub>Si<sub>12</sub> alloys with dimension of 30 mm × 30 mm × 5 mm have been prepared by a combustion synthesis technique [17]. Cylindrical compressive specimens with a gauge length of 4.5 mm and a diameter of 2.8 mm were cut using an electro-discharging machine, and both ends of the compressive specimens were polished to mirror surfaces, and coated with graphite before tests to reduce the interfacial friction. Quasistatic uniaxial compression tests were performed at room temperature using a testing machine with a crosshead speed from  $5.8 \times 10^{-5} \text{ s}^{-1}$  to  $5.8 \times 10^{-2} \text{ s}^{-1}$ . Microstructures of the products after compression tests were examined using a JSM-5600LV scanning electron microscope (SEM). Several specimens after deformation punched from the cross sections of the Fe<sub>88</sub>Si<sub>12</sub> were electro-chemically thinned by twin-jet polishing in an electrolyte of nine parts of methanol and one part of perchloric acid at 243 K and were observed by a JEM-2010 high resolve transmission electron microscope (HRTEM).

## 3. Results and discussion

Fig. 1 shows room temperature compressive engineering stress–strain curves at the different strain rate from  $5.8 \times 10^{-5} \text{ s}^{-1}$

\* Corresponding author. Tel.: +86 931 4968269; fax: +86 931 8277088.  
E-mail address: [tyyflc@163.com](mailto:tyyflc@163.com) (L. Fu).

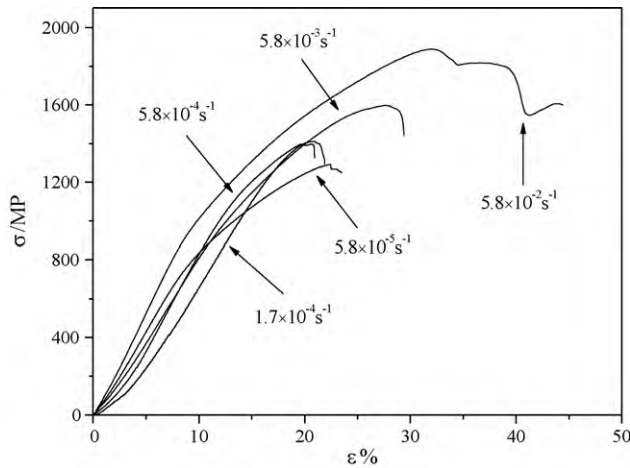


**Fig. 1.** Room temperature compressive engineering stress–strain curves with different strain rates.

to  $5.8 \times 10^{-2} \text{ s}^{-1}$ . The fracture strength of the  $\text{Fe}_{88}\text{Si}_{12}$  is about 1886 MPa at the strain rate of  $5.8 \times 10^{-5} \text{ s}^{-1}$  and the yield strength is 1320 MPa at the strain rate of  $5.8 \times 10^{-2} \text{ s}^{-1}$ , which indicates that the strain rate sensitivity  $m$  (0.018, Fig. 2(a)) is larger than the coarse counterpart. The activity volume  $v^*$ , which was obtained from the strain rate sensitivity  $m$ , is  $6b^3$  on the order of the atomic volume. It indicates that the deformation mechanism is controlled by the dislocation slip [18].

On the other hand, great emphasis has been placed on the breakdown of Hall–Petch scaling at  $d_c$  between 20 nm and 30 nm, which apparently signals a transition from dislocation slip to grain boundary slip in the nanocrystalline metals and alloys. In order to elucidate the deformation behavior of the  $\text{Fe}_{88}\text{Si}_{12}$  alloy, the critical shear stress ( $\tau_c$ ) and the  $d_c$  are calculated, respectively. Taking into account the stress concentrations and the interactions of disloca-

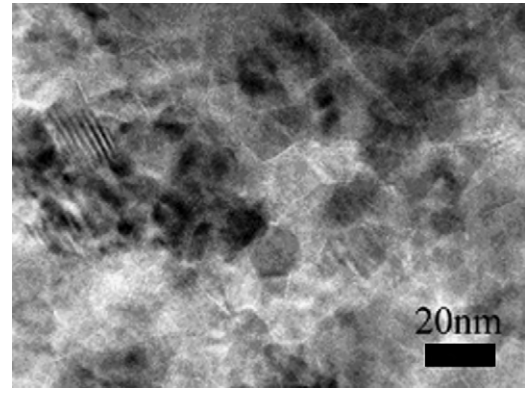


**Fig. 3.** HRTEM image of the nanocrystalline  $\text{Fe}_{88}\text{Si}_{12}$  alloy.

tions with grain boundaries [19], the critical size  $d_c$  is calculated as follows, it is expressed by Talyer dislocation hardening model [20]:

$$\rho = (\gamma/Gb_1)^2(n\alpha b - b_1)^{-2} \quad (1)$$

$$\tau_c = \alpha G b \rho^{1/2} \quad (2)$$

where  $\gamma$  refers to the stacking fault energy (SFE) of metal, while  $b$  and  $b_1$  to the burgers vector of the full and shockley partial dislocation, respectively, and  $G$  to the shear modulus,  $\rho$  to the density of the dislocation,  $\alpha$  reflects the character of the dislocation (0.5 and 1.5) for edge and screw dislocations, respectively [10]. In the case of products, the parameters in Eqs are given as follows:  $\gamma = 38 \times 10^{-3} \text{ J/m}^2$ ,  $G = 81.7 \text{ GPa}$ ,  $b = (\sqrt{2}/2)a$ , where  $a$  is the lattice of  $\text{Fe}_{88}\text{Si}_{12}$ ,  $b_1 = (\sqrt{6}/6)a$ .

Taking  $\alpha = 0.5$  (edge dislocations for multi-phase nanostructure), the  $\tau_c$  is calculated to be 1830 MPa and the  $d_c$  is approximately 5.3 nm for  $\text{Fe}_{88}\text{Si}_{12}$  alloy. The yield strength of 1320 MPa of the bulk nanocrystalline  $\text{Fe}_{88}\text{Si}_{12}$  alloy is lower than

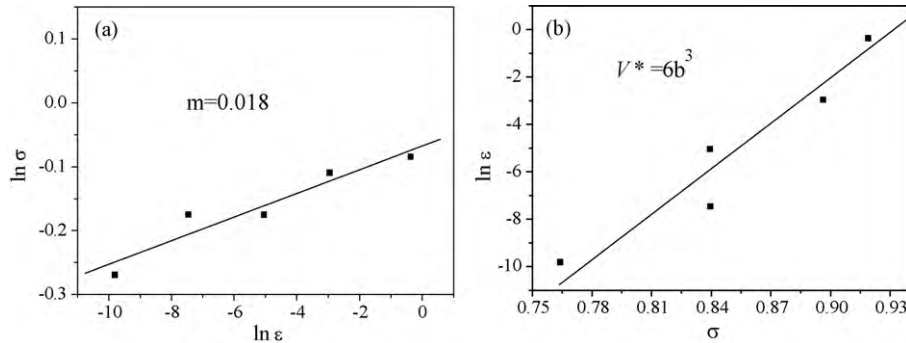


**Fig. 2.** (a) Double logarithmic plot of normalized stress vs. strain rate to determine strain rate sensitivity  $m$ ; (b) plot of flow stress (at 0.5% strain) vs.  $\ln \varepsilon$  to determine the average activation volume  $v^*$  [14] for the nanocrystalline  $\text{Fe}_{88}\text{Si}_{12}$  alloy.

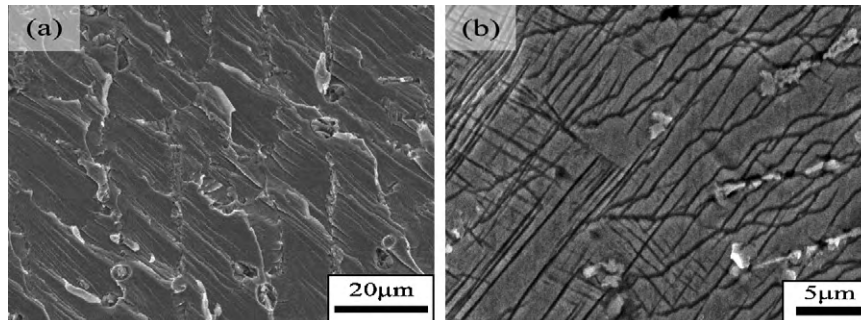


**Fig. 4.** SEM micrographs of the (a) fractured surface, (b) the fractured profile of the nanocrystalline  $\text{Fe}_{88}\text{Si}_{12}$  alloy showing their high-density slip bands.

the  $\tau_c$ , which may be the presence of flaws in the bulk  $\text{Fe}_{88}\text{Si}_{12}$  alloy, such as porosity at nano-scale or trifling of impurities.

The average grain size of the  $\text{Fe}_{88}\text{Si}_{12}$  alloy is about 10 nm from Fig. 3, which is below the critical size apparently. So, the compressive deformation behavior is mainly controlled by dislocation slip. It is further confirmed by Fig. 4 (a) and (b) which shows many slip bands.

The Fe–Si alloys containing less than 10 at.% Si possess only short range atomic order and deform by slip or twinning. At above 10 at.% Si, the alloys possess long range atomic order, and deformation twinning is suppressed in this region, and the deformation occurs entirely by slip. The bulk nanocrystalline  $\text{Fe}_{88}\text{Si}_{12}$  alloy consist of  $\text{DO}_3$   $\text{Fe}_3\text{Si}$  phase and  $\alpha$ -Fe(Si) solid solution phase. These  $\alpha$ -Fe(Si) grains are uniformly distributed into the  $\text{Fe}_3\text{Si}$  matrix (both of the grain size is about 10 nm) [17]. Shin et al. [21] reported that atomic order has a rewarding effect on the dislocation slip deformation behavior of  $\text{Fe}_{88}\text{Si}_{12}$  alloy with the stoichiometric  $\text{Fe}_3\text{Si}$  alloy. The dislocations accumulate in the nano  $\alpha$ -Fe(Si) grains after the compression test start, and then propagate into nano  $\text{Fe}_3\text{Si}$  grains. The high strain hardening rates of the bulk nanocrystalline  $\text{Fe}_{88}\text{Si}_{12}$  alloy have been begotten after yielding by the rapid increase in the back stresses to the propagation of dislocations into  $\text{Fe}_3\text{Si}$  grains. So, the high strength and large strain are obtained.

#### 4. Conclusions

The deformation behavior of the bulk nanocrystalline  $\text{Fe}_{88}\text{Si}_{12}$  alloy, which consists of  $\alpha$ -Fe(Si) and  $\text{Fe}_3\text{Si}$  phases with grain size of 10 nm, has been investigated with compression tests at different strain rates. On one hand, the activity volume  $v^*$  is  $6b^3$ , and on the other hand, the critical size of the nanocrystalline  $\text{Fe}_{88}\text{Si}_{12}$  alloy for deformation mechanism is calculated to be about 5.3 nm, which

is smaller than the grain size of the nanocrystalline  $\text{Fe}_{88}\text{Si}_{12}$  alloy. Both of these show that deformation mechanism of the nanocrystalline  $\text{Fe}_{88}\text{Si}_{12}$  alloy is controlled by dislocation pile-up.

#### Acknowledgements

This work was supported by the National Natural Science Foundation of China (50801064) and the National 973 Project of China (2007CB607601)

#### References

- [1] B.Q. Han, J.Y. Huang, Y.T. Zhu, E.J. Lavernia, Scripta Mater. 54 (2006) 1175–1178.
- [2] J. Eckert, U. Kühn, J. Das, S. Scudino, N. Radtke, Adv. Eng. Mater. 7 (2005) 587–596.
- [3] Y.M. Wang, E. Ma, Acta Mater. 52 (2004) 1699–1709.
- [4] K.S. Kumar, H. Van Swygenhoven, S. Suresh, Acta Mater. 51 (2003) 5743–5774.
- [5] M.A. Tschoppa, D.L. McDowell, Scripta Mater. 58 (2008) 299–302.
- [6] X. Huang, N. Hansen, N. Tsuji, Science 312 (2006) 249–251.
- [7] D. Wolf, V. Yamakov, S. Phillpot, A. Mukherjee, H. Gleiter, Acta Mater. 53 (2005) 1–40.
- [8] M.A. Meyers, A. Mishra, D.J. Benson, Prog. Mater. Sci. 51 (2006) 427–556.
- [9] X.Z. Liao, Y.H. Zhao, S.G. Srinivasan, Y.T. Zhu, Appl. Phys. Lett. 84 (2006) 021909.
- [10] Y. Nakamoto, M. Yuasa, Y. Chen, H. Kusuda, M. Mabuchi, Scripta Mater. 58 (2008) 731–734.
- [11] S. Cheng, J.A. Spencer, W.W. Milligan, Acta Mater. 51 (2003) 4505–4518.
- [12] T.R. Malow, C.C. Koch, Metall. Trans. A 29A (1998) 2285–2295.
- [13] R.J. Asaro, P. Krysly, B. Kad, Phil. Mag. Lett. 83 (2003) 733–743.
- [14] J. Chen, L. Lu, K. Lu, Scripta Mater. 54 (2006) 1913–1916.
- [15] R.J. Asaro, S. Suresh, Acta Mater. 53 (2005) 3369–3382.
- [16] J. Chen, Y.N. Shi, K. Lu, J. Mater. Res. 20 (2005) 2955–2959.
- [17] L.C. Fu, J. Yang, Q.L. Bi, J.Q. Ma, W.M. Liu, Combustion synthesis and characterization of bulk nanocrystalline  $\text{Fe}_{88}\text{Si}_{12}$  alloy. IEEE Trans. Nanotechnol., doi:10.1109/TNANO.2009.2028023.
- [18] J. Lian, C. Gu, Q. Jiang, Z. Jiang, J. Appl. Phys. 99 (2006) 076103.
- [19] A. Gemperle, J. Gemperlová, N. Zárubová, Mater. Sci. Eng. A 387 (2004) 46–50.
- [20] C. Huang, K. Wang, S.D. Wu, Z.F. Zhang, G.Y. Li, S.X. Li, Acta Mater. 54 (2006) 655–665.
- [21] J. Shin, Z. Lee, T.D. Lee, E.J. Lavernia, Scripta Mater. 45 (2001) 725–731.